

Targeted Smooth Bayesian Causal Forests: An analysis of heterogeneous treatment effects for simultaneous versus interval medical abortion regimens over gestation

Jennifer E. Starling*, Jared S. Murray, Patricia A. Lohr,
Abigail R.A. Aiken, Carlos M. Carvalho, and James G. Scott

July 21, 2022

Abstract

This article introduces Targeted Smooth Bayesian Causal Forests, or `tsbcf`, a semi-parametric Bayesian approach for estimating heterogeneous treatment effects which vary smoothly over a single covariate in the observational data setting. The `tsbcf` method induces smoothness in estimated treatment effects over the target covariate by parameterizing each tree's terminal nodes with smooth functions. The model allows for separate regularization of treatment effects versus prognostic effect of control covariates; this approach informatively shrinks towards homogeneity while avoiding biased treatment effect estimates. We provide smoothing parameters for prognostic and treatment effects which can be chosen to reflect prior knowledge or tuned in a data-dependent way.

We apply `tsbcf` to early medical abortion outcomes data from British Pregnancy Advisory Service. Our aim is to assess relative effectiveness of simultaneous versus interval administration of mifepristone and misoprostol over the first nine weeks of gestation, where we define successful outcome as complete abortion requiring neither surgical evacuation nor continuing pregnancy. We expect the relative effectiveness of simultaneous administration to vary smoothly over gestational age, but not necessarily other covariates, and our model reflects this. We demonstrate the performance of the `tsbcf` method on benchmarking experiments. The R package `tsbcf` implements our method.

Keywords and phrases: Bayesian additive regression tree, causal inference, regularization, Gaussian process, heterogeneous treatment effects

*Corresponding author: jstarling@utexas.edu

1 Introduction

Home use of mifepristone and misoprostol to induce abortion in the first nine weeks of gestation is safe and preferable to women over use in the clinic setting (Gold and Chong, 2015; Ngo et al., 2011). However, in England and Wales, the law does not permit use of abortion medications outside of registered medical facilities (Abortion Act, 1967 (c.87)). The current recommended regimen for medical abortion up to 63 days of gestation in Britain is 200 mg oral mifepristone followed by 800 micrograms vaginal misoprostol 24-48 hours later (of Obstetricians and Gynaecologists, 2011). This “interval” protocol requires a minimum of two clinic visits, which imposes financial and logistical burdens on women’s access to medical abortion. Prior research shows that simultaneous dosing of mifepristone and misoprostol is on average 97% as effective as interval administration and is strongly preferred by women (Lohr et al., 2018). British Pregnancy Advisory Services, a non-profit abortion provider with 60 clinics in England and Wales, introduced the option of in-clinic simultaneous dosing in 2015. In the absence of legal home use, simultaneous dosing reduces barriers to access.

Patients choose which regimen they prefer, and practitioners must provide guidance which balances relative effectiveness of the two regimens versus accessibility. A key clinical question is whether the relative effectiveness for simultaneous versus interval administration varies at later gestational ages, for specific subgroups of women, or a combination. Previous work uses logistic regression with propensity score quintiles to adjust for self-selection to treatment protocol, and considers gestation discretized by weeks seven and earlier, week eight, and week nine (Lohr et al., 2018). While this analysis did not find significant decreases in relative effectiveness as gestation advanced, it did not allow for smooth change in effectiveness over gestation, nor does it allow for nuanced subgroup analysis and careful regularization of heterogeneous treatment effects.

Let function $f(t, x, z)$ represent the probability of successfully early medical abortion occurring at gestational age t (in half-weeks), for a patient with maternal covariates x ,

who selected regimen z . Let $z = 1$ be the “treatment”, or simultaneous, and $z = 0$ be the “control”, or interval, regimens. We write this function as the sum of prognostic effect and treatment effect, $f(t, x, z) = \mu(t, x) + \tau(t, x)z$. The first goal of this paper is to formulate a model which provides better estimates of $\tau(t, x)$, when $\tau(t, x)$ evolves smoothly over t but not necessarily x , where the model is carefully regularized to provide unbiased causal estimates for observational data.

The second goal is to apply this model to the early medical abortion data to provide clinicians with accurate, smooth estimates of relative effectiveness over gestation for individual patients and clinically relevant subgroups. This work fills an important gap in ability to assess the relative effectiveness of early medical abortion regimens over time. Current literature does not provide a way to characterize this function which allows for smooth evolution of the treatment effect as gestation progresses. In addition, while clinicians expect that relative effectiveness should evolve smoothly over gestation, there is not strong prior knowledge regarding potential heterogeneity in treatment groups and how that heterogeneity may change over gestation. We apply our model to data from the British Pregnancy Advisory Service to estimate $\tau(t, x)$, providing clinicians with smooth estimates of relative effectiveness over gestation for both individuals, as well as conditional average relative effectiveness estimates for subgroups of patients.

To estimate heterogeneous treatment effects which evolve smoothly over a target covariate (gestation), we propose a new ensemble-of-trees model called Targeted Smooth Bayesian Causal Forests. Our approach is based on the very successful Bayesian Additive Regression Trees (BART) model, introduced by Chipman et al. (2010). Our approach is based on the very successful Bayesian Additive Regression Trees (BART) model, introduced by Chipman et al. (2010). The BART model is a Bayesian tree ensemble model for regression, which predicts scalar response y as the sum of binary regression trees over covariates x . Trees are regularized by a prior to be “weak learners”, i.e. to be shallow with relatively few splits, to avoid overfitting. Our model leverages two BART extensions: the

BART with Targeted Smoothing (tsBART) framework of Starling et al. (2019) and the carefully regularized Bayesian Causal Forests (bcf) model of Hahn et al. (2017). BART with Targeted Smoothing adapts the BART framework to induce smoothness over a single target covariate, and has been shown to outperform regular BART in when the underlying regression function is in fact smooth over this covariate. Bayesian Causal Forests adapts the BART framework to predict heterogeneous treatment effects, and regularizes the prior to avoid biased treatment effect estimation. Motivated by modeling relative effectiveness of early medical abortion regimens over gestation, our tsbcf model builds on the BART framework, extending both aforementioned models in order to model smooth heterogeneous treatment effects for observational data.

In Section 2 we provide an overview of the early medical abortion regimens and the dataset. Section 3 details the tsbcf model and reviews relevant work. Section 4 presents results of a simulation study showing the advantages of tsbcf for several clinically relevant treatment effect scenarios. Section 5 presents results of the early medical abortion analysis using the tsbcf method. Section 6 contains discussion. Section 7 provides supplemental materials; the R package `tsbcf` implements our method. The Appendix provides additional detail on fitting the tsbcf model.

2 Early Medical Abortion Regimens

2.1 Background.

Mifepristone and misoprostol are used together to induce medical abortion through the ninth week of gestation. The recommended regimen for early medical abortion in Britain is 200 mg oral mifepristone, followed by 800 micrograms vaginal misoprostol 24-48 hours later (of Obstetricians and Gynaecologists, 2011). This “interval” protocol requires a minimum of two clinic visits, which imposes financial and logistical burdens on women’s access to medical abortion. British Pregnancy Advisory Services, a non-

profit abortion provider with 60 clinics in England and Wales, introduced the option of in-clinic simultaneous dosing in 2015; in this regimen, mifepristone and misoprostol are administered in a single clinic visit. Simultaneous dosing of mifepristone and misoprostol has been shown to be 97% as effective on average as interval administration, and is strongly preferable; 85% of the women observed chose simultaneous over interval (Lohr et al., 2018). Simultaneous dosing eliminates the need for a second clinic visit, reducing barriers to access.

Patients select which protocol to undertake, and depend on clinicians' guidance as to the relative effectiveness of each choice. Knowledge of whether there is any change in relative effectiveness as gestation progresses, and whether there are subgroups of patients who should be counseled differently, allows clinicians to provide more accurate and personalized information to their patients. Uncertainty quantification is also a key component of providing patients with comprehensive guidance.

Previous research (Lohr et al., 2018) investigates whether relative effectiveness decreases at later gestational ages, and does not find evidence of a significant drop in effectiveness for simultaneous versus interval dosing as gestational age increases. This work uses a logistic regression model with gestational age groups and propensity score quintiles as covariates; gestational age is discretized into 49 days or less, 50-56 days, and 57-63 days. A limitation of this model is the discretization of gestation, as the model does not provide a smooth estimate of the impact of gestational age progress on relative effectiveness. A second limitation is that while inclusion of propensity score estimates may help adjust for biased treatment effect estimates due to self-assignment, the model lacks regularization to reduce bias in the presence of potential targeted selection (Hahn et al., 2018). This model does not allow for exploration of subgroups or nuanced estimation of individual treatment effects over gestation. Our model improves on this previous approach with careful regularization, uncertainty quantification, smoothness over gestational age, and estimates of both subgroup and individual-level relative effectiveness estimates.

2.2 Data description.

We use observational data from early medical abortions provided at British Pregnancy Advisory Service clinics from May 1, 2015 to April 30, 2016. Data was collected from British Pregnancy Advisory Service's electronic booking and invoicing system, which contains records of services provided to clients, including selected demographic and clinical characteristics. These data are initially entered by telephone operators at British Pregnancy Advisory Service's telephone contact center; details are then validated by clinicians at both in-person consultations and at treatment appointments. Complications and adverse outcomes are identified during post-treatment follow-up visits, or British Pregnancy Advisory Services is notified by other providers or by women themselves. When possible, hospital discharge summaries or documents from general practitioners are obtained to confirm outcomes. Staff cross-check the booking and invoicing system for any appointments with British Pregnancy Advisory Services after the date of treatment, and hand-check medical records if a continuing pregnancy or incomplete abortion was recorded in the complications database. This study was approved and exempted from full human subjects review by British Pregnancy Advisory Services and The University of Texas at Austin since all data were pre-existing and were provided in a fully de-identified format.

The dataset consists of 28,895 independent patient records. The sample consists of women with pregnancies of between 4.5 weeks (32 days) 9 weeks (63 days) gestation or less as determined by abdominal or vaginal ultrasonography, who wanted a medical abortion, and who had no contraindications. Early medical abortion is available through 9 weeks of gestation. While 4 weeks is typically the earliest a patient is aware of the pregnancy, only 12 women obtained early medical abortions below 4.5 weeks; our analytic sample begins at 4.5 weeks. Women were offered the choice between 200 mg oral mifepristone followed by 800 micrograms vaginal misoprostol within 15 minutes (simultaneous administration), or 24-72 hours later. Women chose their preferred regimen after

being informed of expected differences in side effects and outcomes. Our analytic sample consists of women who chose simultaneous dosing or a 24-48 hour interval between medications.

The binary response is a successful early medical abortion outcome, defined as complete expulsion of uterine contents after early medical abortion, without surgical intervention and without continuing pregnancy, as defined by the Medical Abortion Reporting of Efficacy Guidelines Creinin and Chen (2016). Women could choose to return two weeks post-treatment for a vaginal ultrasound, or could use a low-sensitivity urine pregnancy test (detection limit 1,000 international units human chorionic gonadotrophin) and symptom checklist to self-report the outcome of the abortion (Cameron et al., 2015). Women could schedule a clinic visit at any time to address concerns or symptoms of a possible complication, including continuing pregnancy. Women diagnosed at a follow-up visit with a retained nonviable sac or embryo were offered the choice of another 800 micrograms vaginal mifepristone or surgical evacuation, and women diagnosed with continued pregnancy were offered surgical evacuation; all of these are considered unsuccessful procedures.

3 Targeted Smooth Bayesian Causal Forests

Targeted Smooth Bayesian Causal Forests (tsbcf) offers a promising technique for estimating relative effectiveness of simultaneous versus interval administration of mifepristone and misoprostol. Suppose that x_i represents available covariates for patient i : maternal age (years), Body Mass Index (kg/m^2), maternal ethnicity (Asian, Black, Other, Not Reported, white), and the numbers of previous abortions, births, Cesarean sections, and miscarriages. Let t_i represent the gestational age at which early medical abortion occurred, in discrete half-week milestones ranging from 4.5 (32 days) to 9 (63 days).

We begin by briefly reviewing the original BART framework on which our method is

Characteristic	(N = 28,895)	Interval: (N = 4,354)	Simultaneous: (N = 24,541)	P-value
Gestational age in weeks, n (%)				< 0.0001
4-5	407 (1.41)	20 (0.46)	387 (1.58)	
5-5.5	4,917 (17.02)	531 (12.20)	4,386 (17.87)	
6-6.5	9,453 (32.72)	1,244 (28.57)	8,209 (33.45)	
7-7.5	7,875 (27.25)	1,368 (31.42)	6,507 (26.51)	
8-8.5	5,577 (19.30)	1,019 (23.40)	4,558 (18.57)	
9	666 (2.30)	172 (3.95)	494 (2.01)	
Maternal age in years, n (%)				= 0.0001
(11,20]	5,312 (18.38)	888 (20.40)	4,424 (18.03)	
(20,30]	15,010 (51.95)	2,178 (50.02)	12,832 (52.29)	
(30,40]	7,695 (26.63)	1,181 (27.12)	6,514 (26.54)	
(40,53]	878 (3.04)	107 (2.46)	771 (3.14)	
Maternal ethnicity, n (%)				< 0.0001
Asian	2,610 (9.03)	510 (11.71)	2,100 (8.56)	
Black	1,839 (6.36)	310 (7.12)	1,529 (6.23)	
Not Reported	537 (1.86)	64 (1.47)	473 (1.93)	
Other	1,568 (5.43)	247 (5.67)	1,321 (5.38)	
White	22,341 (77.32)	3,223 (74.02)	19,118 (77.90)	
BMI, n (%)				= 0.5364
Underweight (<18.5)	2,149 (7.44)	329 (7.56)	1,820 (7.42)	
Normal (18.5-24.9)	14,667 (50.76)	2,209 (50.73)	12,458 (50.76)	
Overweight (25.0-29.9)	7,367 (25.50)	1,080 (24.80)	6,287 (25.62)	
Obese (>30.0)	4,712 (16.31)	736 (16.90)	3,976 (16.20)	
Previous abortions, n (%)				< 0.0001
0	18,354 (63.52)	2,949 (67.73)	15,405 (62.77)	
1-2	9,876 (34.18)	1,301 (29.88)	8,575 (34.94)	
3+	665 (2.30)	104 (2.39)	561 (2.29)	
Previous births, n (%)				< 0.0001
0	18,354 (63.52)	2,949 (67.73)	15,405 (62.77)	
1-2	5,070 (17.55)	609 (13.99)	4,461 (18.18)	
3+	5,471 (18.93)	796 (18.28)	4,675 (19.05)	
Previous Cesarean sections, n (%)				< 0.0001
0	18,354 (63.52)	2,949 (67.73)	15,405 (62.77)	
1-2	1,346 (4.66)	169 (3.88)	1,177 (4.80)	
3+	9,195 (31.82)	1,236 (28.39)	7,959 (32.43)	
Previous miscarriages:				< 0.0001
0	18,354 (63.52)	2,949 (67.73)	15,405 (62.77)	
1-2	2,046 (7.08)	264 (6.06)	1,782 (7.26)	
3+	8,495 (29.40)	1,141 (26.21)	7,354 (29.97)	

Table 1: Descriptive characteristics of women choosing simultaneous or interval administration of mifepristone and misoprostol for early medical abortion. Patients obtained early medical abortion from May 1, 2015 to April 30, 2016 at British Pregnancy Advisory Service clinics. P-values test for differences in distribution of patient characteristics between the simultaneous and interval groups using chi-squared tests.

based (Chipman et al., 2010). We then review BART with Targeted Smoothing (Starling et al., 2019) and Bayesian Causal Forests (Hahn et al., 2017), the two BART extensions we leverage in development of our model. We then introduce our Targeted Smooth Bayesian Causal Forests method, discuss model assumptions and modeling a binary response, followed by a re-

view of relevant literature.

3.1 The BART model.

We begin by reviewing the original Bayesian Additive Regression Trees (BART) model. BART is a Bayesian tree ensemble model for regression, known for accurate prediction while avoiding specification of a parametric model formulation. BART models an unknown function $f(x)$ as the sum of piecewise constant binary regression trees (Figure 1, Left and Middle). The BART model is defined by a likelihood and prior. Each tree T_l , $1 \leq l \leq L$, consists of a set of internal decision nodes which partition the covariate space (A_1, \dots, A_{B_l}) ; each partition element A_b is associated with a terminal node value m_{lb} .

The partition and leaves define a piecewise constant function, $g_l(x) = m_{lb} \forall x \in A_b$. Each of the L regression trees are additively combined into a single estimate $f(x) = \sum_{l=1}^L g_l(x)$. The BART prior constrains the g_l functions to favor small trees and leaf parameters that are close to zero; in this way, trees are “weak” learners, regularizing BART to avoid overfitting. Each tree independently follows the prior described in Chipman et al. (2010), where probability that a node splits at depth h is given by $\eta(1+h)^{-\beta}$ where $\eta \in (0, 1)$ and $\beta \in [0, \text{inf})$. The leaf parameters are given independent priors $m_{lb} \sim N(0, \sigma_m^2)$ with $\sigma_m = \sigma_0/\sqrt{L}$.

Chipman et al. (2010) suggest letting $\eta = 0.95$ and $\beta = 2$ to put low probability on deep trees with many splits. They also suggest using σ_0 to calibrate the possible range of estimated $f(x)$ values, as the induced marginal prior of $f(x)$ is centered at zero with approximately 95% of the prior mass $\pm 2\sigma_0$. Model fitting is accomplished using an MCMC Bayesian Backfitting algorithm; we refer readers to the original paper for full details.

BART has been successful in a variety of contexts including prediction and classification (Chipman et al., 2010; Murray, 2017; Linero and Yang, 2017; Linero, 2018; Hernández et al., 2018), survival analysis (Sparapani et al., 2016; Starling et al., 2019), and causal inference (Hill, 2011; Hahn et al., 2017; Logan et al., 2017; Sivaganesan et al., 2017).

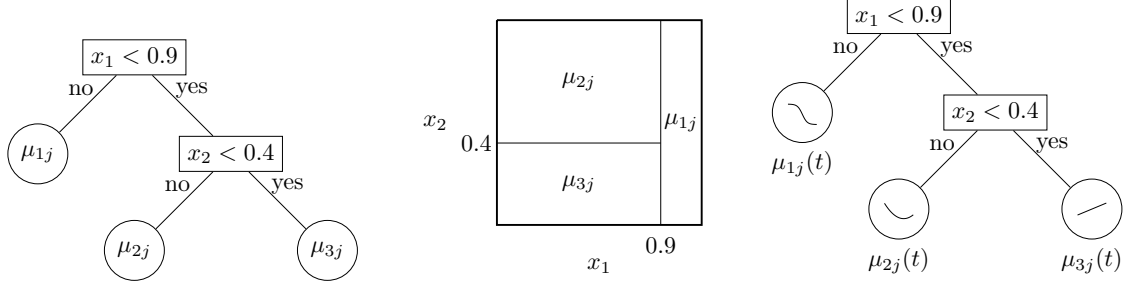


Figure 1: (Left) An example binary tree T_j where terminal nodes are labeled with the corresponding scalar parameters μ_{hj} . (Middle) The corresponding partition of the sample space and the step function $g(T_j, M_j)$. (Right) BART with Targeted Smoothing where the $\mu_{hj}(t)$ parameters associated to terminal nodes are now functions of time t .

3.2 BART with Targeted Smoothing

The BART model is known for excellent predictive performance but lacks smoothness. Starling et al. (2019) introduce a method called BART with Targeted Smoothing (tsBART) for regression that is smooth in some covariate t ; the scalar node-level parameters m_{hj} are replaced with univariate functions $m_{hj}(t)$ and assigned a Gaussian Process prior with a squared-exponential covariance function. Figure 1 (Right) illustrates a single example tree with targeted smoothing. The model formulation for tsBART is similar to BART, except that the estimand $f(t, x)$ is now explicitly a function of covariates and the target covariate. Observations consist of (y_i, t_i, x_i) where x_i is the vector of unsmoothed covariates and t_i is the value of the target covariate. Then the model is formulated as

$$y_i = f(t_i, x_i) + \epsilon_i, \quad \epsilon_i \sim N(0, \sigma) \quad (1)$$

$$f(t_i, x_i) = \sum_{j=1}^m g_j(t_i, x_i; T_j, M_j). \quad (2)$$

The BART with Targeted Smoothing model is fit using intuitive extensions to the Bayesian Backfitting detailed in Chipman et al. (2010), and requires an additional parameter specification: κ , a smoothness parameter, regulates the lengthscale of the Gaussian Process prior. Starling et al. (2019) provide an intuitive default and tuning suggestions for this parameter, while other parameter settings mirror the original BART method.

3.3 Bayesian Causal Forests

Bayesian Causal Forests (bcf) extends the BART framework to estimate heterogeneous treatment effects for observational data (Hahn et al., 2017). Let x represent covariates, and z a binary treatment indicator. Then bcf models response surface $f(x, z)$ as the sum of two functions: a function modeling prognostic impact of control covariates, representing the component of the mean response unrelated to treatment effect, and a second representing the treatment effect directly. The two functions are modeled as separate tree ensembles with their own BART priors, allowing for separate regularization of the treatment effect estimate. This approach allows treatment effect priors to shrink towards homogeneous treatment effects.

The bcf model specifies that the prognostic BART fit includes propensity score estimates as a covariate to improve treatment effect estimation in the presence of confounding. Improvement is particularly pronounced when confounding is due to *targeted selection*, in which individuals select the treatment protocol based on predictions of the potential outcomes (Hahn et al., 2018).

Observations consist of (y_i, z_i, x_i) , where y_i indicates response, z_i binary treatment, and x_i is the vector of covariates. Let $\hat{\pi}(x_i)$ be estimates of the propensity score $P(z_i = 1 | x_i)$. The bcf model is formulated as

$$y_i = f(x_i, z_i) + \epsilon_i, \quad \epsilon_i \sim N(0, \sigma^2) \quad (3)$$

$$f(x_i, z_i) = \mu(x_i, \hat{\pi}(x_i)) + \tau(x_i) z_i \quad (4)$$

where μ and τ are the prognostic and treatment BART fits. The goal is estimating conditional average treatment effects (CATE) – the amount by which response y_i differs in the cases where $z_i = 1$ versus $z_i = 0$, notated using the counterfactual outcomes framework of Imbens and Rubin (2015) where $y_i(0)$ and $y_i(1)$ denote potential outcomes under control versus treatment. In this framework, observations correspond to realized treat-

ments, such that $y_i = z_i y_i(1) + (1 - z_i) y_i(0)$. Then the causal estimand is expressed as $\tau(x_i) = f(x_i, z_i = 1) - f(x_i, z_i = 0)$.

The bcf model has desirable qualities for modeling relative effectiveness of early medical abortion protocols. We could include gestational age in the covariate vector x . However, bcf lacks any mechanism to induce smoothness over gestational age, consistent with clinical intuition.

3.4 Targeted Smooth Bayesian Causal Forests

Let y denote a scalar response, and z a binary treatment indicator. Let x denote a p -length vector of observed control variables, and t a scalar target variable over which we wish to induce smoothness. Consider an observed sample of independent observations (y_i, t_i, z_i, x_i) for $i \in \{1, \dots, n\}$. We introduce Targeted Smooth Bayesian Causal Forests (tsbcf), a method which leverages the frameworks of tsBART and bcf to model heterogeneous treatment effects which vary smoothly over t while providing appropriate regularization to avoid biased treatment effect estimates.

We restrict to the mean-zero additive error setting

$$y_i = f(t_i, x_i, z_i) + \epsilon_i, \quad \epsilon_i \sim N(0, \sigma^2) \quad (5)$$

such that $E(y_i | t_i, x_i, z_i) = f(t_i, x_i, z_i)$ and the treatment effect of letting $z_i = 1$ versus $z_i = 0$ is equivalent to

$$\tau(t_i, x_i) = f(t_i, x_i, 1) - f(t_i, x_i, 0) \quad (6)$$

We then model the response surface $E(y_i | t_i, x_i, z_i) = f(t_i, x_i, z_i)$ as

$$f(t_i, x_i, z_i) = \mu(t_i, x_i, \hat{\pi}_i) + \tau(t_i, x_i, z_i) \quad (7)$$

which allows for direct specification of a prior over the treatment effects. We also include the estimated propensity score in the estimation of the prognostic effect. We use variants of the tsBART prior to model μ and τ .

To model μ , we use the default tsBART prior with 200 trees, depth penalty $\beta = 2$, splitting probability $\eta = 0.95$, and smoothing parameter $\kappa_\mu = 1$, with a half-Cauchy prior on the scale of leaf parameters (Gelman, 2006; Starling et al., 2019). For modeling τ , we prefer the tsBART prior to have stronger regularization to reflect our belief that treatment effect heterogeneity is generally simple over covariates and time. We let $\kappa_\tau = 1$ to reflect heterogeneity over t . We use 50 trees and set $\beta = 3$ and splitting probability $\eta = 0.25$ to shrink towards homogeneity in x . We replace the half-Cauchy prior with a half-Normal prior on the scale of the leaves, with median set to the marginal standard deviation of y .

We assign σ^2 an inverse chi-squared prior, $\sigma^2 \sim \nu\lambda/\chi_\nu^2$. See Appendix A1 for full model specification, including data augmentation to induce the half-Cauchy and half-Normal priors on the respective scales. See Appendix A2 for details on model fitting; we fit the model using updates to the Bayesian Backfitting algorithms for tsBART and bcf. Starling et al. recommend WAIC-based tuning approaches for the tsBART smoothing parameter κ , and similar tuning may be undertaken here in conjunction with intuition and prior knowledge about the likely form of heterogeneity in the treatment effect.

3.5 Assumptions

Throughout the paper, we make the stable unit treatment value (SUTVA) assumption, which excludes interference between units and multiple versions of treatment (Imbens and Rubin, 2015). We also assume that strong ignorability holds, which stipulates that there is no unmeasured confounding so that

$$y_i(0), y_i(1) \perp\!\!\!\perp z_i \mid x_i \tag{8}$$

and there is sufficient overlap to estimate treatment effects everywhere in covariate space such that

$$0 < P((z_i = 1 \mid x_i)) < 1 \tag{9}$$

for all $i \in 1, \dots, n$ observations.

3.6 Modeling a Binary Response

In the original BART paper, Chipman et al. (2010) provide a probit version of the BART model for binary outcomes $Y \in \{0, 1\}$.

$$Pr(Y = 1 \mid x) = \Phi(G(x)) \tag{10}$$

$$G(x) = \sum_{j=1}^m g(x; T_j, M_j) \tag{11}$$

where Φ is the standard normal CDF and $G(x)$ is the standard BART model. Inference is accomplished via data augmentation using the method of Albert and Chib (1993). The tsBART method may be similarly augmented.

The tsbcf model can be extended in the same way for the binary early medical abortion outcomes. Let c_i be the observed binary response for $i \in \{1, \dots, n\}$, with target covariate t_i , treatment indicator z_i , and vector of covariates x_i . Let y_i be the Gaussian latent variable, then similar to the original BART model, we write our model as follows. Let

$$c_i = \begin{cases} 1 & \text{if } y_i \geq 0 \\ 0 & \text{if } y_i < 0 \end{cases}$$

such that $P(c_i = 1 | t_i, x_i) = \Phi(y_i)$, where

$$y_i = \mu(t_i, x_i, \hat{\pi}) + \tau(t_i, x_i, \hat{\pi}_i)z_i + \epsilon, \quad \epsilon_i \sim N(0, 1) \quad (12)$$

Counterfactual probabilities of success are

$$\omega_i(0) = \Phi(\mu(t_i, x_i, \hat{\pi}_i)) \quad (13)$$

$$\omega_i(1) = \Phi(\mu(t_i, x_i, \hat{\pi}_i) + \tau(t_i, x_i)) \quad (14)$$

so for observation i , causal estimands are expressed on the probability scale as

$$\text{Absolute Risk Reduction: } \Delta_i = \omega_i(1) - \omega_i(0) \quad (15)$$

$$\text{Relative Risk: } RR_i = \omega_i(1)/\omega_i(0) \quad (16)$$

$$\text{Number Needed to Treat: } NNT_i = 1/\Delta_i. \quad (17)$$

We include propensity score estimates and covariate vector x_i in estimation of prognostic effects. We refer readers to Rosenbaum and Rubin (1983); Hahn et al. (2017) for a detailed discussion of reasons for including both; briefly, inclusion of propensity score is an effective dimension-reduction technique which yields a prior that flexibly adapts to complex patterns of confounding, and control covariates (instead of only propensity score) are necessary for identifying heterogeneous treatment effects, particularly when we do not believe that the response depends on covariates x strictly through the propensity score.

3.7 Connection with existing work.

Our paper builds on several other extensions to the Bayesian tree-modeling framework. We leverage two papers in particular in formulating the tsbcf model. The first is Hahn

et al. (2017), who propose the Bayesian Causal Forest (bcf) model. Their model estimates heterogeneous treatment effects from observational data using the BART framework, with separately regularized BART priors for prognostic and treatment effects. This approach allows for separate regularization of the treatment effect, allowing for shrinking towards homogeneity. Their method is particularly careful in handling two closely related phenomenon: targeted selection and regularization induced confounding.

Targeted selection occurs when selection into treatment is based in part on expected outcomes under control, $\mu(t, x)$, where the probability of treatment is generally increasing or decreasing as some function of this estimate. (This implies some functional relationship between propensity scores π and expected outcomes under treatment μ .) This seems a likely scenario in the early medical abortion case, where clinicians may be likely to caution patients they perceive as high-risk more strongly about potential decrease in effectiveness of the simultaneous regimen. Additionally, for accessibility reasons, clinicians may provide more conservative advice to patients at more advanced gestational ages.

Estimation of treatment effects is complex because the minimal set of control variables is generally never known, and there are often many candidate control variables. Regularization therefore plays a key role in accurate treatment effect estimation, but in settings with confounding and modest treatment effects, biased treatment effects can occur if regularization is not performed carefully. Hahn et al. (2018) calls this phenomenon “regularization-induced confounding” (RIC); we refer interested readers to their paper and Hahn et al. (2017) for a full discussion. Briefly, RIC characterizes the tendency of regularization priors to over-shrink control variable estimates, which adversely biases treatment effect estimates. The bcf method’s careful specification of regularization priors avoids this phenomenon, and our tsbcf method similarly guards against this bias.

For inducing smoothness in a target covariate, we build on the BART with Targeted Smoothing (tsBART) method (Starling et al., 2019), which replaces trees’ scalar leaf parameters with smooth functions over the target covariate and assigns Gaussian Process priors

over the discrete grid of target covariate values for smoothing. The degree of smoothness is regulated via tuning parameter κ (default value 1) which regulates the lengthscale of the covariance. Our method also uses the Gaussian Process prior to induce smoothness, but allows for separate regularization of the degree smoothness for the prognostic and treatment estimates.

We refer interested readers to Chipman et al. (2010) for a detailed review of the original BART method. Other work has been done on smooth versions of BART, notably Linero and Yang (2017). Linero et al. propose smoothing a regression tree ensemble by randomizing the decision rules at internal nodes of the tree. This model induces smoothness over all covariates by effectively replacing the step function induced by the binary trees with sigmoids, instead of smoothing over one targeted covariate.

4 Simulations

We compare `tsbcf` to several existing models in a benchmarking study designed to simulate five clinically plausible treatment effect scenarios. We generate prognostic effects, treatment effects, and random noise for each scenario, and assess how well each model recovers the treatment effects. We compare the following models.

- **bcf**: The Bayesian Causal Forest model described in Hahn et al. (2017). We expect this model to perform well but lack smoothness (Figure 7).
- **hillbart**: Ordinary BART used to model the response surface in the causal inference setting (Hill, 2011).
- **lm**: A linear model of the form $Y = X\beta + ZX\alpha$ where design matrices X include the target covariate, all other covariates, and two- and three-way interactions between all predictors, including the target covariate.
- **psbart**: Ordinary BART with estimated propensity scores included as a covariate

(Rosenbaum and Rubin, 1983).

- **splines:** A linear model with cubic B-splines with 7 degrees of freedom modeling the target covariate, and two- and three-way interactions among all predictors, including the target covariate splines.
- **tsbcf_default:** The tsbcf method, with smoothing parameters $\kappa_\mu = 1$ and $\kappa_\tau = 1$.
- **tsbcf_wiggly:** The tsbcf method, with smoothing parameters $\kappa_\mu = 1$ and $\kappa_\tau = 3$.

Simulated data is generated as follows. For independent observations $i \in \{1, \dots, n\}$, draw a vector of covariates $x_i = \{x_{1i}, x_{2i}, x_{3i}, x_{4i}, x_{5i}\} \stackrel{iid}{\sim} N(0, 1)$ and draw target covariate $t_i \in \{0.1, 0.2, \dots, 1\}$. Each observation is assigned to treatment ($z_i = 1$) or control ($z_i = 0$) based a binomial draw with propensity score

$$\pi_i = \Phi \left(\rho \cdot \left[\frac{x_{1i}}{6} - \frac{x_{2i}}{4} \right] + (1 - \rho) [-1(x_{4i} > 5) + 1(x_{4i} < 5)] \right) \quad (18)$$

where $\rho \in [0, 1]$ controls the amount of targeted selection; ρ controls the degree to which the propensity score is based on a somewhat accurate prediction of the potential outcome, since $\left[\frac{x_{1i}}{6} - \frac{x_{2i}}{4} \right]$ is found in the prognostic effect (Equation 20), while x_{4i} and x_{5i} are not used in prognostic or treatment effect generation. We generate estimates for the propensity scores $\hat{\pi}_i$ using the **dbarts** R package (Chipman et al., 2010); any accurate prediction is viable, as in Hahn et al. (2017).

We then generate observations as

$$y_i = \mu(t_i, x_{1i}, x_{2i}) + \tau(t_i, x_{3i})z_i + \epsilon_i, \quad \epsilon_i \sim N(0, \sigma^2) \quad (19)$$

where μ is the prognostic function and τ is the treatment effect function. The prognostic

function is the same for all five scenarios:

$$\mu(t_i, x_{1i}, x_{2i}) = 8 + \frac{3}{4}t_i + \frac{x_{1i}}{6} + \frac{x_{2i}}{4} \quad (20)$$

We vary $\tau(t_i, x_i)$ by scenario, reflecting different treatment effects as follows.

- Scenario A represents a treatment effect that varies smoothly over the target covariate t , with homogeneity in x .

$$\tau(t_i, x_i) = 2.5 + 0.75t_i - 0.05 \sin(2\pi t_i)$$

- Scenario B represents heterogeneous treatment effects that vary smoothly over t with modest differences in subgroups.

$$\tau(t_i, x_i) = 2.5 + 1.5\mathbb{I}(x_{3i} > -1/2) + 1.5\mathbb{I}(x_{3i} > 1/2) + 0.75t_i - 0.05 \sin(2\pi t_i)$$

- Scenario C represents heterogeneous treatment effects, similar to Scenario B except that the effects of t and x are inseparable.

$$\tau(t_i, x_i) = 2.5 + 1.5\mathbb{I}(x_{3i} > -1/2) + (1.5 + 0.375t_i)\mathbb{I}(x_{3i} > 1/2) + 0.375t_i - 0.05 \sin(2\pi t_i)$$

- Scenario D gives heterogeneous treatment effects with small effects in general, except for a small subgroup with a pronounced effect.

$$\tau(t_i, x_i) = 0.5 + 0.05\mathbb{I}(x_{3i} > -1/2) + 2.5\mathbb{I}(x_{3i} > 1/2) + 0.75t_i - 0.05 \sin(2\pi t_i)$$

- Scenario E is a constant treatment effect, requiring shrinking to homogeneity in both

x and t .

$$\tau(t_i, x_{3i}) = 3$$

Let $\sigma^2 = 1$ for all scenarios. This setting scales treatment effects to be relatively modest compared to prognostic effects (roughly a third of the magnitude), and scales random noise appropriately to the size of the treatment effects.

Figure 2 illustrates the setup for our benchmarking simulation for a single simulated dataset and provides motivation for the tsbcf method. The five columns represent each scenario, with target covariate tgt on the x-axis, and the conditional average treatment effect (CATE) on the y-axis. In each panel, the solid line(s) represent the ground truth for each scenario's treatment effects; a single line indicates homogeneity in covariates, while multiple lines indicate heterogeneous subgroups. Dashed lines are posterior mean CATE estimates, and shaded regions are 95% posterior credible intervals. While the bcf estimates in the top row are generally good, they lack smoothness in the target covariate, which motivates our method. The tsbcf estimates induce smoothness over the target covariate without compromising the accuracy of the bcf estimates.

Figure 3 gives the average RMSE for recovering the CATE over the target covariate for each model and scenario combination. RMSE is averaged over 100 replications of the simulation, each consisting of generating a dataset and fitting each model. Each row represents a sample size, and each column is a scenario. Within each panel, lines give average RMSE over the target covariate for each method; RMSE is calculated for each replication at each target covariate value, and then the average is calculated across replicates. The tsbcf model performs comparably to the bcf while inducing the desired smoothness that we saw in Figure 2. Results confirm that we have successfully achieved the goal to induce smoothness while not compromising excellent performance. The linear and spline models significantly underperform in scenarios with heterogeneous treatment effects.

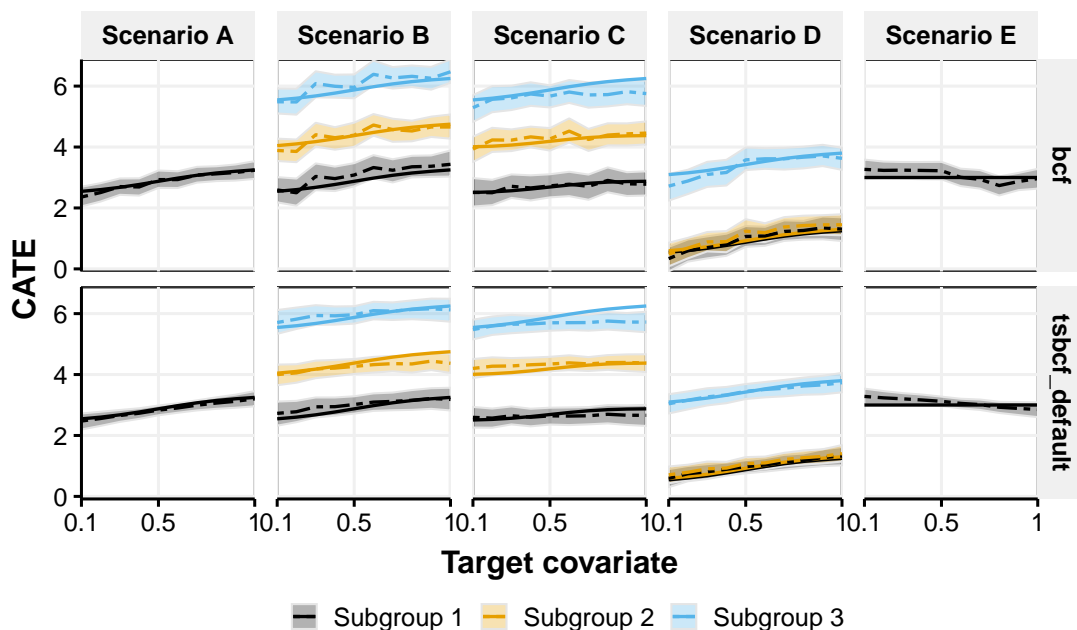


Figure 2: This figure illustrates the setup for our benchmarking simulation and provides motivation for the tsbcf method. We simulate five different clinically plausible treatment effect scenarios. In each panel, the target covariate is on the x-axis and CATE is on the y-axis. In each panel, the solid line(s) represent the ground truth for each scenario’s treatment effects; a single line indicates homogeneity in covariates, while multiple lines indicate heterogeneous subgroups. Dashed lines show posterior mean CATE estimates and shaded regions give 95% posterior credible intervals. The top row shows Bayesian Causal Forest (bcf) estimates for CATE; the bottom row gives estimates using Targeted Smooth Bayesian Causal Forests (tsbcf) with default smoothness parameter settings. While the bcf estimates are generally good, they lack smoothness in the target covariate, which motivates our method. The tsbcf estimates induce smoothness over the target covariate without compromising the accuracy of the bcf estimates.

We next focus on methods with smaller RMSE (Figure 3) and inspect RMSE for recovering CATE in relation to coverage and interval length. Panel A gives coverage versus RMSE; the lower-right corner of the plot gives the optimal frontier of low RMSE combined with good coverage. All of the methods maintain approximately nominal (95%) coverage, while the tsbcf methods have lower RMSE. The “default” tsbcf outperforms the “wiggly” version here, as the true treatment effects are very smooth over the target covariate; however, the “wiggly” version is still outperforming other methods. Panel B gives coverage versus interval length. Both tsbcf settings have slightly narrower inter-

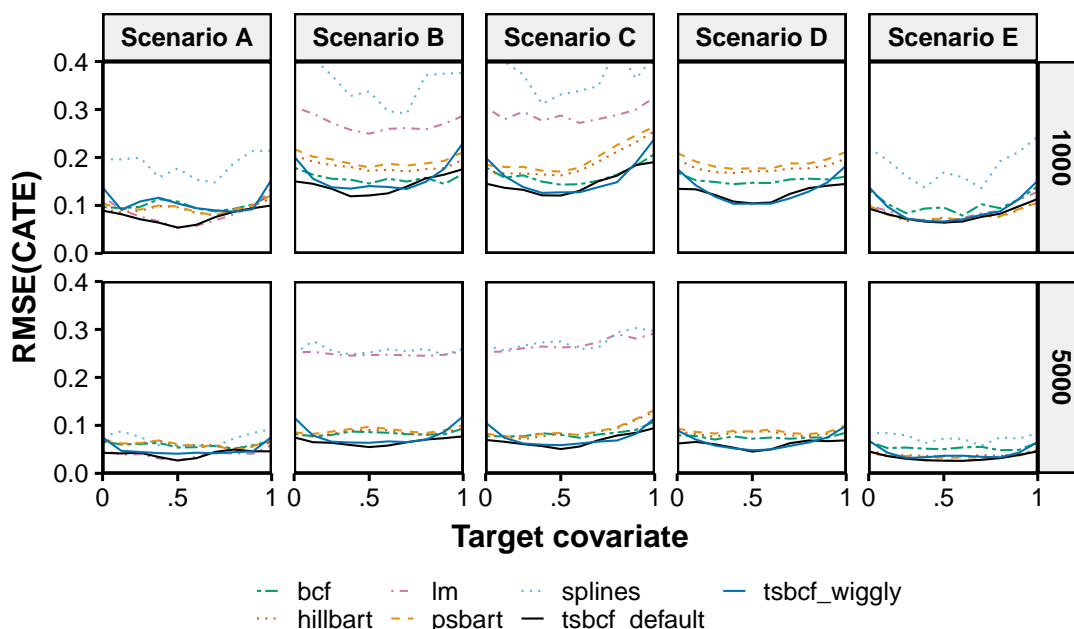


Figure 3: RMSE for recovering the conditional average treatment effects (CATE) for subgroups in each scenario across the target covariate. RMSE is averaged over 100 replicates of the simulation, each consisting of generating a dataset and fitting the models. The rows give results for two sample sizes. We compare several models; `tsbcf_default` and `tsbcf_wiggly` are `tsbcf` with default ($\kappa_\mu = 1, \kappa_\tau = 1$) and less smooth ($\kappa_\mu = 1, \kappa_\tau = 3$) settings. Both `tsbcf` models perform comparably to the `bcf` model while inducing the desired smoothness. Results confirm that we have achieved the goal to induce smoothness while not compromising accurate heterogeneous treatment effect estimation. The linear and spline model estimates are biased due to generation of the simulation with some confounding, to mimic realistic observational data scenarios; regular BART methods are less robust to this confounding, while `bcf` and `tsbcf` are designed to be robust due to separate regularization of the treatment tree fit.

vals than other methods, and `bcf` has slightly inflated variance due to lack of smoothness over the target covariate. Panel C gives interval length versus RMSE, and `tsbcf` has both shortest interval length and lowest RMSE, for both smoothness settings. Together, these panels demonstrate that in scenarios where the underlying treatment effect is smooth over the target covariate, `tsbcf` recovers the heterogeneous treatment effects while maintaining coverage and yielding reasonable measures of uncertainty.

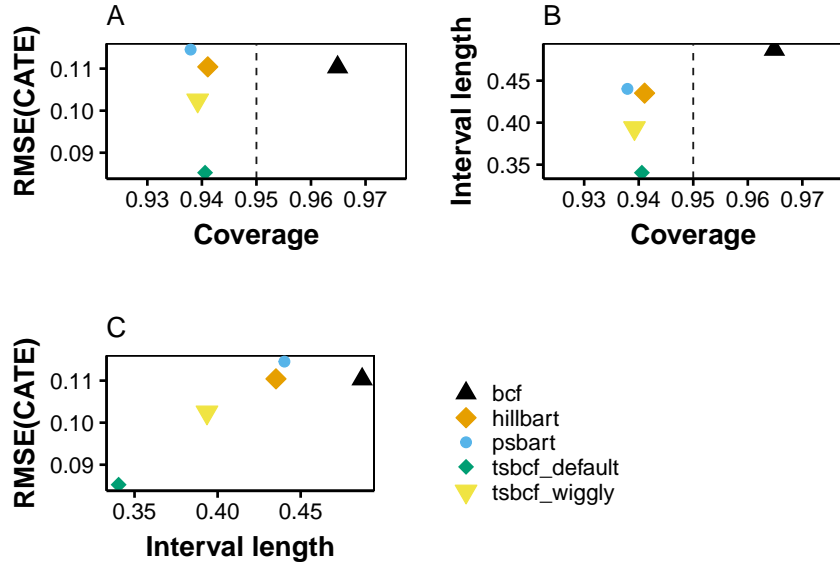


Figure 4: Compares average RMSE, coverage, and interval length for each method. (A) Coverage versus RMSE, where the lower-right frontier gives the optimal frontier of low RMSE combined with good coverage. All methods maintain approximately nominal (95%) coverage while the tsbcb methods have lower RMSE. The “default” tsbcb outperforms the “wiggly”, as the true treatment effects are very smooth over the target covariate; however, the “wiggly” version is still outperforming other methods. (B) Coverage versus interval length. Both tsbcb settings have slightly narrower intervals than other methods, and bcf has slightly inflated variance due to lack of inducing smoothness over the target covariate. (C) Interval length versus RMSE, and tsbcb has both shortest interval length and lowest RMSE for both smoothness settings. Together, these demonstrate that in scenarios where the underlying treatment effect is smooth over the target covariate, tsbcb recovers the heterogeneous treatment effects while maintaining coverage and yielding reasonable measures of uncertainty.

5 Results for Early Medical Abortion Modeling

We now focus on our scientific problem, estimating relative effectiveness of simultaneous versus interval administration of mifepristone and misoprostol in early medical abortion. We apply tsbcb to the British Pregnancy Advisory Services data described in Section 2. We model the probability of successful early medical abortion across gestational age, $\tau(t, x)$, using the probit extension of the tsbcb (Section 3.6). Our target covariate for smoothing is gestational age in half-weeks, $t_i \in \{4.5, 5, 5.5, \dots, 9\}$, where 4.5 indicates 32–34 days gestation, 5 weeks indicates 35–38 days, 5.5 indicates 39–41 days, and so on. Let

c_i be a binary indicator for successful early medical abortion, and z_i be a binary indicator for simultaneous ($z_i = 1$) versus interval ($z_i = 0$) regimen. Let x_i be the vector of patient characteristics, including age in years, body mass index (kg/m^2), maternal ethnicity, and numbers of previous abortions, births, Cesarean sections, and miscarriages.

Our goal is to provide clinicians with a smooth estimate of relative effectiveness of simultaneous versus interval protocols across gestational age, to provide accurate advice to women selecting a protocol. We are interested in knowing average relative effectiveness across gestation, as well as whether there are subgroups of patients where relative effectiveness over gestation differs. Relative effectiveness is calculated as the ratio between the two counterfactual treatment effect estimates on the probability scale. Let y_i be the probit latent variables as in Equation 12. Then the counterfactual probabilities of successful emergency medical abortion are as defined in Equations 12 and 13, and causal estimands relative risk and number needed to treat are as in Equation 15. We refer to relative risk as “relative effectiveness” of the simultaneous compared to interval protocol throughout our work, as defining a “risk” of successful procedure is not clinically intuitive; there is no mathematical distinction.

For each MCMC iteration (b), we obtain a draw of $\Delta_i^{(b)}$ and $RR_i^{(b)}$ for each patient at each gestational age; we can then average across patients at each gestational age to obtain each MCMC draw of the Δ and RR for a given gestation, or average across subgroups of patients to obtain MCMC draws of the Δ and RR for that subgroup at a given gestation. We summarize results by calculation posterior mean and 95% credible intervals at each gestational age. For MCMC draws $b \in \{1, \dots, B\}$, $RR_i^{(b)}$ is the b^{th} MCMC draw for relative risk for individual i who is observed at gestational age t_i . Then we obtain posterior draws of estimated relative effectiveness at some gestational age t as

$$\hat{RR}_t^{(b)} = \sum_{i|t_i=t} \hat{RR}_i^{(b)} \quad (21)$$

then we use MCMC draws $\{\hat{RR}_t^{(1)}, \dots, \hat{RR}_t^{(B)}\}$ to calculate the posterior mean and credible interval for RR_t .

We fit the tsbcf model to the early medical abortion data and calculate posterior mean relative effectiveness at each half-week of gestation. Mean posterior relative effectiveness of 0.95 at some gestational age t is clinically interpreted as the simultaneous protocol being 95% as effective as the interval protocol on average at gestational age t . Figure 5, panel A gives posterior mean relative effectiveness of the simultaneous versus interval regimen, averaged across all women, as a function of gestational age. The solid line gives the posterior mean relative effectiveness, and the shaded area reflects 95% posterior credible intervals across gestation. The slight kick-up and inflated credible intervals at nine weeks gestation are a result of small sample size; women obtaining early medical abortion in the ninth week of gestation account for only 2.3% of cases (Table 1).

Number needed to treat (NNT) gives the number of women who would need to be treated under the simultaneous protocol instead of interval before one additional failed procedure is observed than would occur under interval administration. Figure 5, panel B gives the posterior mean NNT and 95% credible interval. While there is a slight decrease in relative effectiveness as gestation advances, the average relative effectiveness remains high over the course of gestation. We also note the large interval including zero at 4.5 weeks; the posterior relative risk is close to 1 here, with credible interval bounds falling on each side of one, indicating that simultaneous and interval protocols are nearly equally effective this early in gestation.

After averaging over the cohort, we aim to identify subgroups of women with heterogeneity in relative effectiveness. We take a “fit-the-fit” approach to subgroup analysis (Hahn et al., 2017) where we use individual relative effectiveness estimates are used as

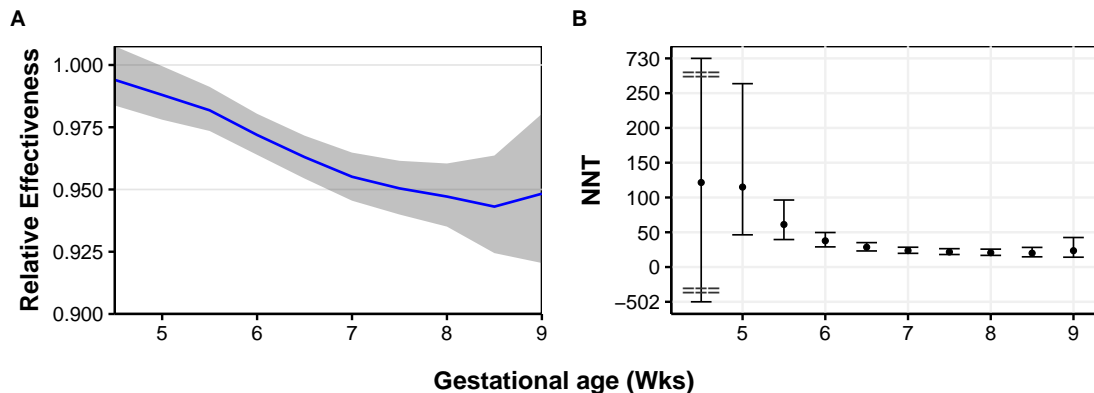


Figure 5: Mean relative effectiveness and number needed to treat for the cohort. (A) Posterior mean relative effectiveness of the simultaneous versus interval regimen, averaged across all women, across gestational age. The solid line gives the posterior mean relative effectiveness, with shaded 95% credible intervals. We note the relatively small sample size at 9 weeks, resulting in a slight kick-up that we do not believe is clinically relevant, as well as inflated uncertainty (Table 1). (B) Posterior mean number needed to treat (NNT), giving the average number of patients needed to receive treatment under the simultaneous regimen before one additional early medical abortion failure is observed compared to failures under the interval regimen. While there is a slight decrease in relative effectiveness as gestation advances, the average relative effectiveness remains high over the course of gestation.

the response. Individual posterior mean relative effectiveness estimates are calculated as

$$\hat{RR}_i = \sum_{b=1}^B \hat{RR}_i^{(b)}. \quad (22)$$

To assess subgroup heterogeneity, we focus on women where gestational age is in the 7–9 week range; this is the clinically interesting area of the posterior mean relative effectiveness curve in Figure 5. The individual relative effectiveness estimates, \hat{RR}_i , for women where $t_i \in 7, \dots, 9$ are used as inputs to a CART model Chipman et al. (1998), with x_i as covariates.

Figure 6 gives the tree fit from the CART model. Each tree node in the figure contains the posterior mean relative effectiveness and the percent of observations for that node. In parenthesis below each terminal node is the NNT corresponding to the relative effectiveness. Age, the first split, is the most important subgroup; patients 29 and older have

slightly lower relative effectiveness compared to their younger counterparts. Within the older and younger cohorts, number of previous births also decreases relative effectiveness, though slightly less so in the younger group of patients.

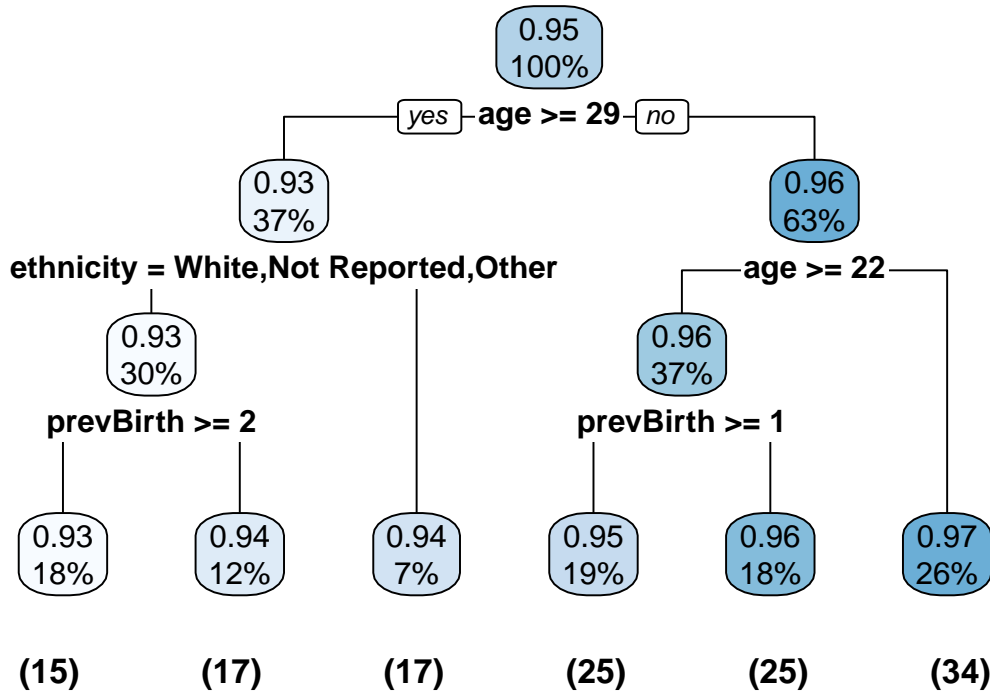


Figure 6: Tree from the “fit-the-fit” CART model to investigate subgroups, where response is individual relative effectiveness estimate, and covariates are patient characteristics. Each node contains the posterior mean relative effectiveness and the percent of observations contained in that split or terminal node. In parenthesis below each terminal node is the NNT corresponding to that node’s relative effectiveness. Age is first split, and so the most important subgroup; patients 29 and older see somewhat decreased relative effectiveness compared to their younger counterparts. Within the older and younger groups of patients, number of previous births also decreases relative effectiveness, though slightly less so in the younger group of patients.

The CART fit gives point estimates of mean posterior relative effectiveness for each node. We query the posterior draws for subgroups at each level of the CART tree. Less overlap in the posterior densities indicates meaningful splits. Concentration of the posterior densities indicates more precisely isolated subgroups as a result of the tree split, and more dispersion indicates greater heterogeneity within a tree split subgroup. Figure 7 plots the posteriors for various splits, moving down the tree. We refer to terminal nodes

of this CART tree as Leaves 1 to 6, from left to right.

Panel A gives posteriors for the first split, on maternal age below 29. The lack of overlap in the posterior relative effectiveness in older and younger women indicates a substantive difference, with older women experiencing lower relative effectiveness than their younger counterparts. Panel B gives posterior distributions for the younger cohort (Leaves 4, 5, and 6). Leaf 4 includes patients ages 22 to 28 with no previous births. Leaf 5 is comprised of patients ages 22 to 28 with one or more previous births, and Leaf 6 includes patients 21 and younger. While there is some overlap between these three subgroups, the posterior for Leaf 4 is noticeably lower than the others. Panel C gives posterior distributions for the second split on the left branch of the tree (splitting on maternal ethnicity). Patients in Leaf 3 are Asian or Black, while patients in Leaves 1 and 2 are white or have ethnicity of Other or Not Reported; all are age 29 or older. These groups do not appear to be substantively different from each other. Panel D considers posteriors for all three leaves on the left side of the tree. Women in Leaf 1 are 29 or older, ethnicity White, Not Reported, or Other, and have two or more previous births. Women in Leaf 2 are same, except for having one or no previous births. Women in Leaf 3 are Asian or Black. Women in Leaf 1 have somewhat lower relative effectiveness than women in Leaves 2 and 3.

To summarize, age split at 29 is an important subgroup, with somewhat decreased relative effectiveness in the older cohort. Within the younger and older cohorts, presence of previous births had a slight negative impact on relative effectiveness, which was more pronounced in patients 29 and older, less in patients 22–28, and not present in patients under 22.

In order to get a better understand the difference in relative effectiveness between subgroups in terms of patient impact, Figure 8 gives a histogram of differences in subgroup average NNT for women age 29 or older with ethnicity white, Other, or Not Reported, and two or more previous births versus women under 22 (Leaf 6). These subgroups correspond to comparing Leaf 1 and Leaf 6 of the CART tree (Figure 6). The histogram plots

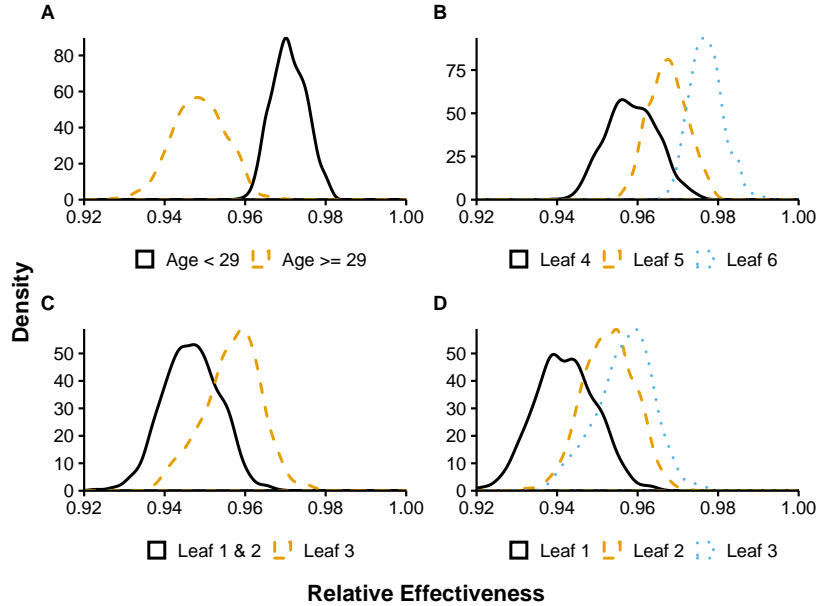


Figure 7: Posterior distributions of relative effectiveness for each CART tree split from Figure 6. We reference terminal nodes 1 to 6, from left to right. Visualizing tree split posteriors gives insight into magnitude of differences subgroups of patients. (A) Splits on maternal age below 29. Lack of overlap in the posterior relative effectiveness in older and younger women indicates a substantive difference in relative effectiveness. (B) Leaf 4 includes patients ages 22 to 28 with one or more previous births. Leaf 5 is comprised of patients ages 22 to 28 with one or more previous births, and Leaf 6 includes patients 21 and younger. The posterior for Leaf 4 is somewhat lower than the others. (C) Splitting on ethnicity in the older cohort. Patients in Leaf 3 are Asian or Black, while patients in Leaves 1 and 2 are white or have ethnicity of Other or Not Reported; all are age 29 or older. These groups do not appear to be substantively different from each other. (D) PPosterior for all three leaves on the left side of the tree. Women in Leaf 1 appear to have somewhat lower relative effectiveness than women in Leaves 2 and 3. In summary, age is the most important covariate defining subgroups, with a split at age 29. Within each age group, previous births decrease relative effectiveness slightly.

the distribution of subgroup average NNT difference for each MCMC draw. Differences generally range from 20 to 60 patients, with no mass at zero, indicating that the difference in these subgroups translates to real differences in number of women at later gestational ages (7–9 weeks) who would need to receive the simultaneous protocol instead of interval before seeing one additional failed procedure.

Figure 9 shows scatterplots of posterior mean relative effectiveness for individual women, by age (panel A) and by number of previous births (panel B). Previous analy-

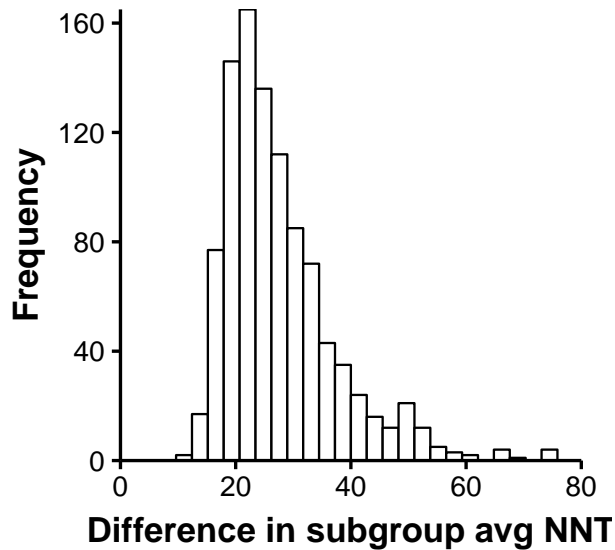


Figure 8: Histogram of MCMC draws of differences in subgroup average NNT for women age 29 or older, with ethnicity white, Other, or Not Reported, and two or more previous births versus women under 22. These subgroups correspond to comparing Leaf 1 and Leaf 6 of the CART tree (Figure 6). Differences generally range from 20 to 60 patients, with no mass at zero, indicating that the difference in these subgroups translates to real differences in number of women who would need to receive the simultaneous regimen instead of interval before seeing an additional failed procedure.

sis focused on averaging over the cohort or subgroups; these scatterplots show the full range of individual posterior relative effectiveness, as well as trends in age and previous birth consistent with Figures 6 and 7. The impact of age on relative effectiveness is stronger than that of previous births, however, increase in each covariate decreases relative effectiveness. Table 2 provides detail on cohort characteristics by posterior relative effectiveness, for women with estimates below 0.90, from 0.90–0.95, and above 0.95. Visualizing individual estimated relative effectiveness gives clinicians confidence that there are not smaller subgroups of patients undetected by our subgroup analysis where relative effectiveness is drastically lower.

Subgroup analysis has identified age and number of previous births as important covariates in predicting relative effectiveness. Partial dependence plots (Figure 10) give average marginal effect of both predictors on relative effectiveness over gestational age.

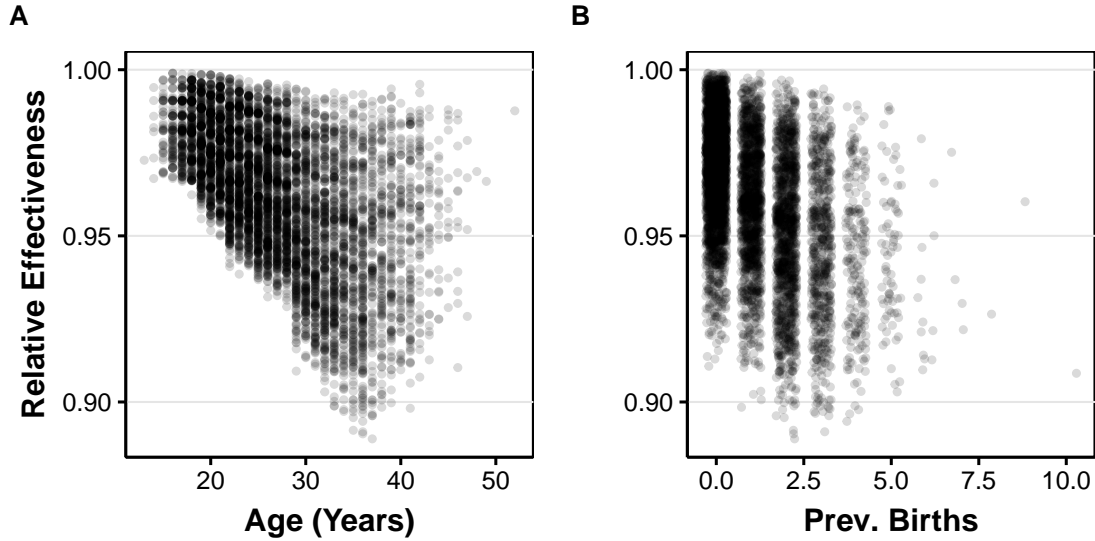


Figure 9: Individual posterior mean relative effectiveness by age (A) and number of previous births (B). Scatterplots show the full range of individual posterior relative effectiveness as well as trends in age and previous birth consistent with Figures 6 and 7. The impact of age on relative effectiveness is stronger than that of previous births, however, increase in each covariate decreases relative effectiveness. There are only a handful of patients whose estimates for relative effectiveness are below 0.90. Table 2 provides detail on cohort characteristics by posterior relative effectiveness, for women with estimates below 0.90, from 0.90–0.95, and above 0.95.

Gestational age is on the x-axis, with lines for age groups and previous number of births. Panel A shows partial dependence of relative effectiveness on age over gestation, grouped by the CART tree splits on age (Figure 7). Panel B shows partial dependence of relative effectiveness on number of previous births. Plots support previous subgroup analysis findings.

The early medical abortion analysis uses our suggested default parameter settings for smoothness parameters ($\kappa_\mu = 1$ and $\kappa_\tau = 1$). We discuss parameter tuning in Section 3; here, we perform a sensitivity analysis for robustness of our analysis to smoothness parameter choice. We let $\kappa_\mu=1$ and fit the tsbcf model to the early medical abortion dataset three times, with $\kappa_\tau \in \{\frac{1}{3}, 1, 3\}$. These choices represent a three-times changes in magnitude in each direction, corresponding to varying the length-scale of the treatment trees' covariance from one to three to nine.

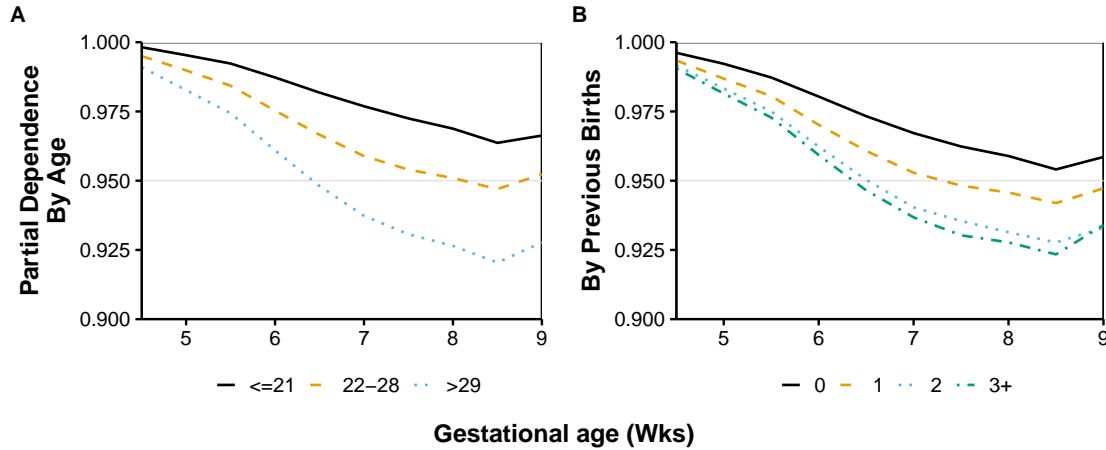


Figure 10: Partial dependence plots for covariates identified in subgroup analysis. These are two-dimensional partial dependence plots, over the respective covariates and gestational age. Gestational age is on the x-axis, with lines for age groups and previous number of births. (A) Partial dependence of relative effectiveness on age over gestation, grouped by the CART tree splits on age (Figure 7). (B) Partial dependence of relative effectiveness on number of previous births. Plots show that the marginal effect of both covariates are consistent with the subgroup analysis.

Figure 11 plots the posterior mean relative effectiveness for three settings of the tsbcf model’s smoothness parameter for the treatment tree fit. The solid line matches Figure 5, giving posterior relative effectiveness over gestational age with shaded 95% posterior credible interval. The dashed lines corresponding to varying the κ_τ smoothness parameter. While there are small differences in the overall estimated relative effectiveness, we do not see clinically meaningful variation from varying the smoothness, indicating that our analysis is robust to smoothing parameter choice. We also note small differences in the 9-week range of gestation, lending support to our intuition that the small increase at 9 weeks is due to small sample size.

Finally, in addition to helping clinicians provide better advice to each patient, clinics must plan appropriately for potential adjustments in staffing and resource needs when providing the simultaneous regimen as an option. To this end, we look at the treatment effect on the treated – for patients who selected the simultaneous regimen and experienced a failure, we plot the distribution of differences in the observed number of failures under simultaneous compared to the expected failures had those patients selected inter-



Figure 11: Posterior mean relative effectiveness for three settings of the tsbcf model’s smoothness parameter for the treatment tree fit. The early medical abortion analysis was performed using the recommended default smoothness parameter settings (1 for both tree fits). The solid line matches Figure 1, giving posterior relative effectiveness over gestational age with shaded 95% posterior credible interval. We fit the same model twice more, setting the treatment tree fit’s smoothness parameter κ_τ to $1/3$ (“smoother”) and 3 (“wigglier”), reflecting shift in magnitude of three times in each direction. We do not see clinically meaningful differences in the three posterior mean estimates across gestation, indicating robustness to choice of smoothness parameter.

val over MCMC draws. We report this on the order of expected additional surgeries per thousand patients, giving clinics a sense of the volume of likely additional procedures. We find that a clinic can expect approximately 40–60 additional surgeries per thousand patients (Figure 12).

6 Discussion

Our Targeted Smooth Bayesian Causal Forests model is a novel model which allows for estimation of heterogeneous treatment effects which evolve smoothly over a target covariate in the observational data setting. Targeted Smooth Bayesian Causal Forests enjoys similar advantages to Bayesian Causal Forests: excellent recovery of heterogeneous treatment effects in observational data, mitigation of biased treatment effect estimates via

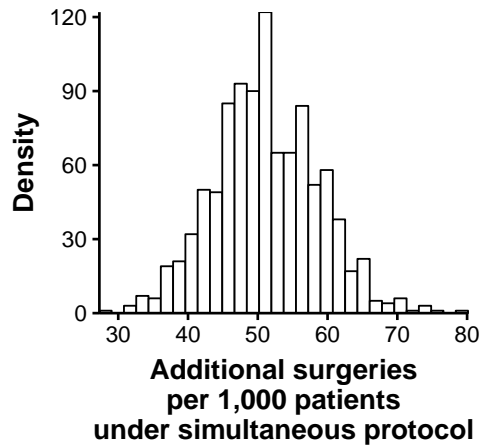


Figure 12: Distribution of differences in observed failure under the simultaneous protocol versus expected failure under interval, for patients selecting simultaneous who experienced failure. Clinics choosing to offer simultaneous administration may anticipate an additional 40-60 surgeries per 1,000 patients treated.

separate regularization of the treatment tree fit, easily tunable hyperparameters, and no need to specify a parametric forms of interactions. Tsbcb also benefits from the smoothness over a single covariate provided by Gaussian Process priors, and has easily tunable hyperparameters to control degree of smoothness via length-scale of the covariance functions, leveraging the Targeted Smooth BART prior introduced by Starling et al. (2019). Other hyperparameters are set efficiently using data-driven approaches as recommended in Hahn et al. (2017) and Chipman et al. (2010). Additionally, like the previously mentioned BART-based methods, tsbcb handles is invariant to transformation of predictors, categorical predictors seamlessly, and mitigates the curse of dimensionality via regularization.

The analysis of relative effectiveness of the simultaneous medical abortion protocol versus interval protocol represents a substantial advancement on previous work (Lohr et al., 2018), in robust handling of potential confounding, smoothness over gestational age, and assessing subgroups of patients with modest amounts of heterogeneity at later gestational ages. We validate the results of Lohr et al. (2018) in that on average, we do not see substantial decrease as gestationl progresses, only very modest decrease after seven

Characteristic	(N = 28,895)	RE >0.95 (N = 21,304)	RE 0.90-0.95 (N = 7,565)	RE <.90 (N = 26)	P-value
Gestational age in weeks, n (%)					< 0.0001
4.5	407 (1.41)	407 (1.91)	0 (0.00)	0 (0.00)	
5-5.5	4,917 (17.02)	4,917 (23.08)	0 (0.00)	0 (0.00)	
6-6.5	9,453 (32.72)	8,430 (39.57)	1,023 (13.52)	0 (0.00)	
7-7.5	7,875 (27.25)	4,583 (21.51)	3,291 (43.50)	1 (3.85)	
8-8.5	5,577 (19.30)	2,605 (12.23)	2,947 (38.96)	25 (96.15)	
9	666 (2.30)	362 (1.70)	304 (4.02)	0 (0.00)	
Maternal age in years, n (%)					< 0.0001
(11,20]	5,312 (18.38)	5,312 (24.93)	0 (0.00)	0 (0.00)	
(20,30]	15,010 (51.95)	12,011 (56.38)	2,999 (39.64)	0 (0.00)	
(30,40]	7,695 (26.63)	3,485 (16.36)	4,185 (55.32)	25 (96.15)	
(40,53]	878 (3.04)	496 (2.33)	381 (5.04)	1 (3.85)	
Maternal ethnicity, n (%)					< 0.0001
Asian	2,610 (9.03)	1,941 (9.11)	669 (8.84)	0 (0.00)	
Black	1,839 (6.36)	1,700 (7.98)	139 (1.84)	0 (0.00)	
Not Reported	537 (1.86)	400 (1.88)	137 (1.81)	0 (0.00)	
Other	1,568 (5.43)	1,165 (5.47)	402 (5.31)	1 (3.85)	
White	22,341 (77.32)	16,098 (75.56)	6,218 (82.19)	25 (96.15)	
BMI category (kg/m ²), n (%)					< 0.0001
Underweight (<18.5)	2,149 (7.44)	1,716 (8.05)	433 (5.72)	0 (0.00)	
Normal (18.5-24.9)	14,667 (50.76)	10,878 (51.06)	3,769 (49.82)	20 (76.92)	
Overweight (25.0-29.9)	7,367 (25.50)	5,179 (24.31)	2,182 (28.84)	6 (23.08)	
Obese (>30.0)	4,712 (16.31)	3,531 (16.57)	1,181 (15.61)	0 (0.00)	
Previous abortions, n (%)					< 0.0001
0	18,354 (63.52)	14,373 (67.47)	3,980 (52.61)	1 (3.85)	
1-2	9,876 (34.18)	6,546 (30.73)	3,306 (43.70)	24 (92.31)	
3+	665 (2.30)	385 (1.81)	279 (3.69)	1 (3.85)	
Previous births, n (%)					< 0.0001
0	18,354 (63.52)	14,373 (67.47)	3,980 (52.61)	1 (3.85)	
1-2	5,070 (17.55)	3,071 (14.42)	1,989 (26.29)	10 (38.46)	
3+	5,471 (18.93)	3,860 (18.12)	1,596 (21.10)	15 (57.69)	
Previous Cesarean cections, n (%)					< 0.0001
0	18,354 (63.52)	14,373 (67.47)	3,980 (52.61)	1 (3.85)	
1-2	1,346 (4.66)	801 (3.76)	545 (7.20)	0 (0.00)	
3+	9,195 (31.82)	6,130 (28.77)	3,040 (40.19)	25 (96.15)	
Previous miscarriages:					< 0.0001
0	18,354 (63.52)	14,373 (67.47)	3,980 (52.61)	1 (3.85)	
1-2	2,046 (7.08)	1,082 (5.08)	948 (12.53)	16 (61.54)	
3+	8,495 (29.40)	5,849 (27.45)	2,637 (34.86)	9 (34.62)	

Table 2: Descriptive characteristics by ranges of posterior mean individual relative effectiveness. Relative effectiveness is divided into three columns: > 0.95, 0.90 – 0.95, and < 0.90. P-values test for differences in distribution of patient characteristics between the three ranges of relative effectiveness. Only 26 women (0.09%) have estimated relative effectiveness less than 0.90; all are over 30, and all but one have at least one previous birth. Additionally, 21,304 women (74%) have estimated relative effectiveness greater than 0.95. Women in the 0.90–0.95 category are also predominantly over 30.

weeks' gestation to a degree which should not make clinicians uncomfortable recommending the simultaneous regimen given its lower barriers to access. Our subgroup identification expands on previous findings; while the simultaneous regimen remains generally very effective, clinicians may wish to use our findings to inform advice to patients age 29 and greater who seek early medical abortion later in gestation (7–9 weeks), particularly those with two or more previous births.

One limitation of our work is the limited set of available covariates. It is plausible that unobserved confounders exist, and our method regularizes to guard against this bias; however, more demographic information about patients may inform subgroup analysis. As described in Lohr et al. (2018), we do not know what covariates influenced each woman’s choice in protocol. Women received counseling on the expected differences in effectiveness and side effects based on a small pilot study conducted by British Pregnancy Advisory Services. We do not know if or how counseling impacted women’s choice in protocol, and aside from clinicians’ use of a common comparison table in a printed client guide, counseling is not standardized. Nonetheless, our work presents a clearer and more nuanced picture of relative effectiveness of simultaneous administration of mifepristone and misoprostol than previously available.

7 Supplemental Materials

The Targeted Smooth Bayesian Causal Forests R package **tsbcf** can be found at <https://github.com/jestarling/tsbcf/>.

REFERENCES

- Abortion Act. Available at <http://www.legislation.gov.uk/ukpga/1967/87/contents>, retrieved June 14, 2017., 1967 (c.87).
- J. H. Albert and S. Chib. Bayesian Analysis of Binary and Polychotomous Response Data. *Journal of the American Statistical Association*, 88(422):669–679, 1993.
- S. Cameron, A. Glasier, A. Johnston, H. Dewart, and A. Campbell. Can women determine the success of early medical termination of pregnancy themselves? *Contraception*, 91:6–11, 2015.
- H. A. Chipman, E. I. George, and R. E. McCulloch. Bayesian CART Model Search. *Journal of the American Statistical Association*, 93(443):935–948, 1998.
- H. A. Chipman, E. I. George, and R. E. McCulloch. BART: Bayesian additive regression trees. *The Annals of Applied Statistics*, 4(1):266–298, 03 2010.
- M. Creinin and M. Chen. Medical abortion reporting of efficacy: the mare guidelines. *Contraception*, 94:97103, 2016.

- A. Gelman. Prior distributions for variance parameters in hierarchical models (comment on article by Browne and Draper). *Bayesian Analysis*, 1(3):515–534, 2006.
- M. Gold and E. Chong. If we can do it for misoprostol, why not for mifepristone? the case for taking mifepristone out of the office in medical abortion. *Contraception*, 92:194-6, 2015.
- P. R. Hahn, J. S. Murray, and C. M. Carvalho. Bayesian regression tree models for causal inference: regularization, confounding, and heterogeneous effects. *arXiv:1706.09523*, 2017.
- P. R. Hahn, C. M. Carvalho, D. Puelz, and J. He. Regularization and Confounding in Linear Regression for Treatment Effect Estimation. *Bayesian Analysis*, 13(1):163–182, 03 2018.
- B. Hernández, A. Raftery, and e. a. Pennington, S.R. Bayesian Additive Regression Trees using Bayesian model averaging. *Stat Comput*, 28:869, 2018.
- J. L. Hill. Bayesian Nonparametric Modeling for Causal Inference. *Journal of Computational and Graphical Statistics*, 20(1):217–240, 2011.
- G. Imbens and D. Rubin. Causal inference in statistics, social, and biomedical sciences. *Cambridge University Press*, 2015.
- A. Linero and Y. Yang. Bayesian Regression Tree Ensembles that Adapt to Smoothness and Sparsity. *arXiv:1707.09461v1 [stat.ME]*, 2017.
- A. R. Linero. Bayesian Regression Trees for High-Dimensional Prediction and Variable Selection. *Journal of the American Statistical Association*, 2018.
- B. R. Logan, R. Sparapani, R. E. McCulloch, and P. W. Laud. Subgroup finding via Bayesian additive regression trees. *Statistical Methods in Medical Research*, 0(0):1–15, 2017.
- P. A. Lohr, J. E. Starling, J. G. Scott, and A. R. Aiken. Simultaneous compared with interval medical abortion regimens where home use is restricted. *Obstetrics and Gynecology*, 2018.
- J. S. Murray. Log-Linear Bayesian Additive Regression Trees for Categorical and Count Responses. *arXiv preprint arXiv:1701.01503*, 2017.
- T. Ngo, M. Park, H. Shakur, and C. Free. Comparative effectiveness, safety, and acceptability of medical abortion at home and in a clinic: a systematic review. *Bull World Health Organ*, 89:360-70, 2011.
- R. C. of Obstetricians and Gynaecologists. The care of women requesting induced abortion. *London (UK): RCOG*, 2011.
- M. T. Pratola, H. A. Chipman, J. R. Gattiker, D. M. Higdon, R. McCulloch, and W. N. Rust. Parallel Bayesian Additive Regression Trees. *Journal of computational and graphical statistics: a joint publication of American Statistical Association, Institute of Mathematical Statistics, Interface Foundation of North America*, 23(3):830–852, 2014. ISSN 1061-8600.
- P. Rosenbaum and D. Rubin. The central role of the propensity score in observational studies for causal effects. *Biometrika*, 70(1):41–55, 04 1983.
- S. Sivaganesan, P. Muller, and B. Huang. Subgroup finding via Bayesian additive regression trees. *Statistics in Medicine*, 36:2391–2403, 2017.

Sparapani, Logan, MucCulloch, and Laud. Nonparametric survival analysis using Bayesian Additive Regression Trees (BART). *Statistics in Medicine*, 35(16):2741–2753, 2016.

J. Starling, J. Murray, C. Carvalho, R. Bukowski, and J. Scott. Bart with targeted smoothing: An analysis of patient-specific stillbirth risk. *Annals of Applied Statistics*, 2019.

8 Appendix

A1. Fitting the tsbcf model.

Here we provide details on the model parameterization and prior for tsbcf. The model is comprised of the sum of two tsBART fits, each with its own prior specification. The model can be written in full as

$$y_i = \mu(t_i, x_i, \hat{\pi}_i) + \tau(t_i, x_i) z_i + \epsilon_i, \quad \epsilon_i \sim N(0, \sigma^2) \quad (23)$$

where the prognostic tsBART fit is parameterized as in Starling et al. (2019).

$$\begin{aligned} \mu(t_i, x_i, \hat{\pi}_i) &= \eta_\mu f_\mu(t_i, x_i, \hat{\pi}_i) \sim \text{tsBART} \\ f_\mu(t_i, x_i, \hat{\pi}_i) &= \sum_{j=1}^{200} g_\mu(t_i, x_i, \hat{\pi}_i; T_{\mu j}, M_{\mu j}), \quad M_{\mu j} \in \{m_{1j}(t), \dots, m_{bj}(t)\} \\ m_{hj} &\sim \text{GP}(0, C_{\theta_\mu}(t, t')) \\ \eta_\mu &\sim N(s_\mu, \gamma^2) \\ \gamma^2 &\sim \text{IG}\left(\frac{1}{2}, \frac{1}{2}\right) \end{aligned}$$

We calibrate the induced half-Cauchy prior’s median s_μ by setting it equal to the twice the marginal standard deviation of y . The variance of the squared exponential GP kernel is set to $1/200$, and smoothness parameter $\kappa_\mu = 1$ governs the length-scale (Starling et al., 2019). The prior on trees $T_{\mu j}$ is as in Chipman et al. (2010), with depth penalty $\beta = 2$ and split probability $\alpha = 0.95$.

For the treatment effect fit, we parameterize to ensure the treatment effect is invariant

to transformation, such that

$$\begin{aligned}
\tau(t_i, x_i) &\sim \text{tsBART} \\
\tau(t_i, x_i) z_i &= [b_1 z_i + b_0 (1 - z_i)] f_\tau(t_i, x_i) \\
f_\tau(t_i, x_i) &= \sum_{j=1}^{200} g_\tau(t_i, x_i, \hat{\pi}_i; T_{\tau j}, M_{\tau j}), \quad M_{\tau j} \in \{m_{1j}(t), \dots, m_{bj}(t)\} \\
m_{hj} &\sim \text{GP}(0, C_\theta(t, t')) \\
b_1 &\sim N\left(\frac{s_b}{2}, \frac{1}{2}\right) \\
b_0 &\sim N\left(-\frac{s_b}{2}, \frac{1}{2}\right)
\end{aligned}$$

This parameterization induces the prior $b_1 - b_0 \sim N(s_b, 1)$ and we set s_b to the marginal median of y . The prior on trees $T_{\tau j}$ uses depth penalty $\beta = 3$ and split probability $\alpha = 0.25$. The variance of the squared exponential GP kernel is set to $1/50$, and smoothness parameter $\kappa_\tau = 1$ governs the length-scale.

The prior for σ^2 follows Chipman et al.'s recommendation for a rough over-estimation of $\hat{\sigma}$. We choose $\nu = 3$ and $q = 0.90$, and estimate $\hat{\sigma}$ by regressing y onto x (including the target variable as a covariate), then choose λ s.t. the q th quantile of the prior is located at $\hat{\sigma}$, i.e. $P(\sigma \leq \hat{\sigma}) = q$.

A2. Bayesian Backfitting Algorithm

We leverage the Bayesian backfitting MCMC algorithms of tsBART and bcf to design a Bayesian backfitting algorithm for tsbcf. We refer interested readers to Chipman et al. (2010) for a full discussion of the original Bayesian backfitting, and Starling et al. (2019) and Hahn et al. (2017) for tsBART and bcf algorithms respectively. Briefly, Bayesian backfitting involves an MCMC algorithm where each tree, and its parameters are sampled one at a time given the partial residuals from the other $m - 1$ trees. One iteration of the sampler consists of looping through the trees, sampling each tree T_j via a Metropolis step, and then sampling its associated leaf parameters M_j , conditional on σ^2 and the remaining trees and leaf parameters. After a pass through all trees, σ^2 is updated in a Gibbs step.

Updating trees and leaves

In general, to sample $\{T_j, M_j\}$ conditioned on the other trees and leaf parameters $\{T_{(j)}, M_{(j)}\}$, define the partial residual as

$$r_{ij} = y_i - \sum_{k=1, k \neq j}^m g(x_i; T_k, M_k). \quad (24)$$

Using r_j as the working response vector, at step s of the MCMC one samples $T_j^{(s)}$ by proposing one of four local changes to $T_j^{(s-1)}$, marginalizing analytically over M_j . The local change is selected randomly from the following candidates:

- **grow** randomly selects a terminal node and splits it into two child nodes
- **prune** randomly selects an internal node with two children and no grandchildren, and prunes the children, making the selected node a leaf
- **change** randomly selects an internal node and draws a new splitting rule
- **swap** randomly selects a parent-child pair of internal nodes and swaps their decision rules

The **change** and **swap** moves are computationally expensive; in practice, BART is often implemented with only **prune** and **grow** proposals (Pratola et al., 2014). Once the move in tree space is either accepted or rejected, M_j is sampled from its Gaussian full conditional, given T_j and σ^2 .

Distributional relationships

Our algorithm for fitting tsbcf retains the form of the method used in bcf, extended to the multivariate setting as in tsBART. The following distributional relationships are useful for deriving the full conditional distributions used in the backfitting updates.

- For $\mu(t_i, x_i, \hat{\pi})$ the "data" is $\left(\frac{y_i - [b_1 z_i + b_0(1-z_i)]\tau(t_i, x_i, \hat{\pi}_i)}{\eta_\mu} \right)$ with variance $\left(\frac{\sigma^2}{\eta_\mu^2} \right)$
- For $\tau(t_i, x_i, \hat{\pi})$ the "data" is $\left(\frac{y_i - \eta_\mu \mu(t_i, x_i, \hat{\pi}_i)}{[b_1 z_i + b_0(1-z_i)]} \right)$ with variance $\left(\frac{\sigma^2}{[b_1 z_i + b_0(1-z_i)]^2} \right)$
- For η_μ the "data" is $\prod_{i=1}^n \text{N} \left(\frac{y_i - [b_1 z_i + b_0(1-z_i)]\tau(t_i, x_i, \hat{\pi}_i)}{\mu(t_i, x_i, \hat{\pi}_i)} \middle| \eta_\mu, \frac{\sigma^2}{\mu(t_i, x_i, \hat{\pi}_i)^2} \right)$
- For b_1 the "data" is $\prod_{i=1}^{n_{z=1}} \text{N} \left(\frac{y_i - \eta_\mu \mu(t_i, x_i, \hat{\pi}_i)}{\tau(t_i, x_i, \hat{\pi}_i)} \middle| b_1, \frac{\sigma^2}{\tau(t_i, x_i, \hat{\pi}_i)^2} \right)$ for only the $z_i = 1$ observations.
- For b_0 , same as b_1 , using only the $z_i = 0$ observations.

Note that we use y_i generally here; for updating tree and leaf parameters $\{T_{\mu j}, M_{\mu j}\}$ and $\{T_{\tau j}, M_{\tau j}\}$ respectively, we are using the partial residuals with all other trees and leaf parameters held constant as described above. For updating the prognostic fit $\mu(t_i, x_i, \hat{\pi})$

$$r_{ij} = y_i - \sum_{k=1, k \neq j}^{200} g(x_k; T_{\mu k}, M_{\mu k})$$

and similarly, for updating the treatment fit $\tau(t_i, x_i, \hat{\pi})$, the "data" consist of the partial residuals

$$r_{ij} = y_i - \sum_{k=1, k \neq j}^{50} g(x_k; T_{\tau k}, M_{\tau k})$$

Full conditionals

The posterior conditional distributions for the Bayesian backfitting algorithm are as follows. For simplicity we assume that target covariate values t are on a common discrete grid, though this is not a requirement.

For updating $(\sigma^2 | \dots)$, the prior, likelihood, and full conditional distributions are

- Prior:

$$p(\sigma^2) \sim \text{IG}\left(\frac{\nu}{2}, \frac{\nu\lambda}{2}\right)$$

- Likelihood:

$$p(y | \sigma^2) = \prod_{i=1}^n \text{N}(y_i | \eta_\mu \mu(t_i, x_i, \hat{\pi}_i) + [b_1 z_i + b_0(1 - z_i)] \tau(t_i, x_i, \hat{\pi}_i), \sigma^2)$$

- Full conditional:

$$p(\sigma | \dots) \sim \text{IG}\left(\frac{\nu + n}{2}, \frac{\sum_{i=1}^n (y_i - \hat{y}_{it}) + \nu\lambda}{2}\right).$$

For updating $(\gamma_\mu^2 | \dots)$, the prior, likelihood, and full conditional distributions are

- Prior:

$$p(\gamma_\mu^2) \sim \text{IG}\left(\frac{1}{2}, \frac{1}{2}\right),$$

- Likelihood:

$$p(\eta_\mu | s_\mu, \gamma_\mu^2) \sim \text{N}(\eta_\mu | s_\mu, \gamma_\mu^2)$$

- Full conditional:

$$p(\gamma_\mu^2 | \dots) \sim \text{IG}\left(1, \frac{(\eta_\mu - s_\mu)^2 - 1}{2}\right).$$

For updating $(b_1 | \dots)$, the prior, likelihood, and full conditional distributions are

- Prior:

$$p(b_1) \sim N\left(\frac{s_b}{2}, 1\right),$$

- Likelihood:

$$p(y | \dots) = \prod_{i=1}^{n_{z=1}} \text{N} \left(\frac{r_i - \eta_\mu \mu(t_i, x_i, \hat{\pi}_i)}{\tau(t_i, x_i, \hat{\pi}_i)} \middle| b_1, \frac{\sigma^2}{\tau(t_i, x_i, \hat{\pi}_i)^2} \right),$$

- Full conditional:

$p(b_1 | \dots) \sim N(m^*, v^*)$, where

$$v^* = \left(\frac{1}{\gamma_b^2} + \frac{1}{\sigma^2} \sum_{i=1}^{n_{z=1}} \tau(t_i, x_i, \hat{\pi}_i)^2 \right)^{-1} \quad \text{and} \quad m^* = v^* \left(\frac{s_b}{\gamma_b^2} + \frac{1}{\sigma^2} \sum_{i=1}^{n_{z=1}} \tau(t_i, x_i, \hat{\pi}_i)^2 r_i \right)$$

For updating $(b_0 | \dots)$, the prior is $p(b_1) \sim N(-\frac{s_b}{2}, 1)$, and the likelihood is computed using the control observations, as opposed to treatment. The full conditional is then similar to that of b_1 .

For updating $(\eta_\mu | \dots)$, the prior, likelihood, and full conditional distributions are

- Prior:

$$p(\eta_\mu) \sim N(s_\mu, \gamma_\mu^2),$$

- Likelihood:

$$p(y | \dots) = \prod_{i=1}^n \text{N} \left(\frac{r_i - [b_1 z_i + b_0 (1 - z_i)] \tau(t_i, x_i, \hat{\pi}_i)}{\mu(t_i, x_i, \hat{\pi}_i)} \middle| \eta_\mu, \frac{\sigma^2}{\mu(t_i, x_i, \hat{\pi}_i)^2} \right)$$

- Full conditional:

$p(\eta_\mu | \dots) \sim N(m^*, v^*)$, where

$$v^* = \left(\frac{1}{\gamma_\mu^2} + \frac{\sum_{i=1}^n \mu(t_i, x_i, \hat{\pi}_i)^2}{\sigma^2} \right)^{-1} \quad \text{and} \quad m^* = v^* \left(\frac{s_\mu}{\gamma_\mu^2} + \frac{1}{\sigma^2} \sum_{i=1}^n \mu(t_i, x_i, \hat{\pi}_i) r_i \right)$$

For updating $\mu(t_i, x_i, \hat{\pi}_i)$ and $\tau(t_i, x_i)$, the priors are tsbcf; updates are performed via the Bayesian backfitting algorithm, using the partial residuals as described previously. For updating prognostic trees $T_{\mu j}$, the marginal likelihood uses homogeneous variances, similar to the marginal likelihood in tsBART. For updating treatment trees $T_{\tau j}$, the marginal likelihood is similar, but for heterogeneous variances. See the following sections for further detail.

8.0.1 Marginal likelihood for prognostic tree updates

The marginal likelihood for updating the prognostic tree fits $\mu(t_i, x_i, \hat{\pi}_i)$ is the homogeneous version from BART with Targeted Smoothing. We derive the marginal log-likelihood here for a single leaf. In the Backfitting algorithm, this is calculated for multiple

leaves depending on whether a birth move or death move is proposed for the tree. The likelihoods are then used in calculating the acceptance probability for the Metropolis step.

Let y_l represent the length n_l vector of residuals for a given leaf. Let $T_{\mu j}$ be the tree structure for the j th tree, and t_{len} be the length of the grid of unique target values. We integrate out leaf means vector m_l to obtain the marginal log-likelihood as follows.

$$p(y_l|T_j, \sigma^2) = \int_{\mathbb{R}} N_{n_l}(y_l|W_l m_l, \sigma^2 I) \cdot N_{t_{\text{len}}}(m_l|m_0, \Sigma_0) \partial m_l$$

where W_l is a $n \times t_{\text{len}}$ matrix, with one row for each observation; all entries are zero, except a 1 in the column corresponding to each observation i 's associated time t_i . Set $m_0 = 0$. The marginal log-likelihood is then

$$p(y_l|T_{\mu j}, \sigma^2) = -\frac{n_l}{2} \log(2\pi\sigma^2) + \frac{1}{2} \log(|K|) - \frac{1}{2} \log(|C|) - \frac{1}{2} \left[\frac{1}{\sigma^2} y_l^T y_l + \mu_0^T K \mu_0 - b^T C^{-1} b \right]$$

where $C = (\frac{1}{\sigma^2} W_l^T W_l + K)$ and $b = (\frac{1}{\sigma^2} W_l^T y_l + K m_0)$. For computational purposes, $W_l^T W_l = [n_1 \dots n_{t_{\text{max}}}]$, the vector of sample sizes for each time. In addition, $y_l^T y_l = \sum_{i=1}^{n_l} y_i$, the sum of all y_i in leaf l .

8.0.2 Marginal likelihood for treatment tree updates

The marginal likelihood for updating treatment fits is slightly more complex. We need the marginal log-likelihood in the case of heterogeneous variances. Recall that for updating $\tau(t_i, x_i, \hat{\pi}_i)$, the variance is $\left(\frac{\sigma^2}{[b_1 z_i + b_0(1-z_i)]^2} \right)$, which is unique for each observation.

Let y_l represent the length n_l vector of residuals for a given leaf. Let $T_{\tau j}$ be the tree structure for the j th tree. We integrate out leaf means vector m_l to obtain the marginal log-likelihood as follows. Instead of $\sigma^2 I = (\omega I)^{-1}$, use the $(n_l \times n_l)$ precision matrix $\Lambda = \text{diag}[\omega_1, \dots, \omega_{n_l}]$.

We integrate out leaf means vector m_l to obtain the marginal log-likelihood as follows.

$$p(y_l|T_{\tau j}, \sigma^2) = \int_{\mathbb{R}} N_{n_l}(y_l|W_l m_l, \Lambda^{-1}) \cdot N_T(m_l|m_0, K^{-1}) \partial m_l$$

where W_l is gain a $n \times t_{\text{len}}$ matrix, with one row for each observation; all entries are zero, except a 1 in the column corresponding to each observations i 's associated time t_i . We again let $\mu_0 = 0$. The marginal log-likelihood is then

$$p(y_l|T_{\tau j}, \sigma^2) = -\frac{n_l}{2} \log(2\pi) + \frac{1}{2} [\log(|\Lambda|) + \log(|K|) - \log(|C|) - [y_l^T \Lambda y_l - b^T C^{-1} b]]$$

where $C = (W_l^T \Lambda W_l + K)$ and $b = (W_l^T \Lambda y_l + K \mu_0)$. For computational purposes, $W_l^T \Lambda W_l$ is the the $t_{\text{len}} \times t_{\text{len}}$ diagonal matrix of sums of precisions for each sample size. $W_l^T \Lambda y_l$ is the vector of $\omega_i y_i$ sums for each time point, and $y_l^T \Lambda y_l = \sum_{i=1}^{n_l} \omega_i y_i^2$. Finally, $\log(|\Lambda|) = \sum_{i=1}^{n_l} \log(\omega_i)$